Deep Blue Oxadiazole-Containing Thermally Activated Delayed Fluorescence Emitters For Organic Light-Emitting Diodes

Michael.Y. Wong,[a‡] Simonas Krotkus,[b‡] Graeme Copley,[a] Wenbo Li,[b] Caroline Murawski,[b] David Hall,[a,b] Gordon Hedley,[b] Marie Jaricot,[a] David B. Cordes,[a] Alexandra M. Z. Slawin,[a] Yoann Olivier,[c] David Beljonne,[c] Luca Muccioli,[d] Monica Moral,[e,f] Juan Carlos Sancho-Garcia,[e] Malte C. Gather,[b] Ifor D. W. Samuel,[b] and Eli Zysman-Colman*[a]*

[a] Organic Semiconductor Centre, EaStCHEM School of Chemistry, University of St Andrews, St Andrews, Fife, UK, KY16 9ST, Fax: +44-1334 463808; Tel: +44-1334 463826; E-mail: eli.zysman-colman@st-andrews.ac.uk;
[b] Organic Semiconductor Centre, SUPA, School of Physics and Astronomy, University of St Andrews, North Haugh, St Andrews, Fife, KY16 9SS, UK, E-mail: idws@st-andrews.ac.uk
[c] Laboratory for Chemistry of Novel Materials, University of Mons, 7000, Mons, Belgium.
[d] Laboratoire de Chimie des Polymères Organiques, UMR 5629, University of Bordeaux, 33607, Pessac, France
[e] Renewable Energy Research Institute, University of Castilla-La Mancha. Paseo de la Investigación 1, 02071, Albacete, Spain.
[f] Department of Physical Chemistry, University of Alicante, 03080, Alicante, Spain
URL: http://www.zysman-colman.com

[‡] co-first author

Keywords: thermally activated delayed fluorescence, organic light emitting diodes, oxadiazoles, blue emitters, DFT calculations

Abstract

A series of four novel deep blue to sky blue thermally activated delayed fluorescence (TADF) emitters (**2CzdOXDMe**, **2CzdOXD4MeOPh**, **2CzdOXDPh** and **2CzdOXD4CF$_3$Ph**) have been synthesized and characterized. These oxadiazole-based emitters demonstrated bluer emission compared with reference emitter **2CzPN** thanks to the weaker acceptor strength of

oxadiazole moieties. The oxadiazole compounds doped in hosts (mCP and PPT) emitted from 435-474 nm with photoluminescence quantum yields ranging from 14%-55%. The emitters possess singlet-triplet excited state energy gaps (ΔE_{ST}) between 0.25 and 0.46 eV resulting in delayed components ranging from 4.8 to 25.8 ms. The OLED device with **2CzdOXD4CF$_3$Ph** shows a maximum external quantum efficiency of 11.2% with a sky-blue emission at CIE of (0.17, 0.25) while the device with **2CzdOXD4MeOPh** shows a maximum external quantum efficiency of 6.6% with a deep-blue emission at CIE of (0.15, 0.11).

Introduction

In organic light-emitting diodes (OLEDs), light is produced through radiative decay of electrically generated excitons. As a function of spin statistics, 75% of the excitons are triplets and 25% of the excitons are singlets. In order to obtain efficient electroluminescent (EL) devices, 100% of the excitons need to be harvested within the emissive layer of the device.[1-2] The current state-of-the-art emitters for OLEDs rely on neutral iridium(III) and platinum(II) complexes as, (1) the emission color of these materials can be easily tuned as a function of ligand design, (2) these complexes possess microsecond emission lifetimes and, most importantly, (3) the heavy metal mediates an efficient intersystem crossing (ISC) to harness both singlets and triplets in OLED devices.[3-7] Despite internal quantum efficiencies (IQE)[5] approaching 100%, these organometallic emissive materials are costly and toxic and, importantly, there exists no stable and bright deep blue emitter, a key component for both displays and lighting applications.[8-9]

As a response to the drawbacks of phosphorescent organometallic emitters, thermally activated delayed fluorescent (TADF)[10-14] materials have recently come to the fore, as they too

are capable of recruiting 100% of the excitons because the energy gap between the lowest singlet (S_1) and triplet (T_1) levels, (ΔE_{ST}), is small enough to permit reverse intersystem crossing (RISC) between the two states at ambient temperature.[15] Compounds possessing small ΔE_{ST} possess structures wherein the highest occupied molecular orbital (HOMO) is spatially separated from the lowest unoccupied molecular orbital (LUMO) in order to minimize the exchange integral between the two.[15-17] Importantly, most TADF emitters are based on either cheap complexes mostly derived from copper[18-24] or are purely organic in nature.[15,25-29]

One of the grand challenges remaining in emitter design for OLEDs is the development of stable and bright *deep-blue* emitters (CIE x,y coordinates each < 0.2),[8,14,30-33] as only limited examples of *deep-blue* TADF emitters have been reported to date. The first organic deep-blue TADF emitters, reported by Zhang *et al.* in 2012, were based on a diphenylsulfone (DPS) acceptor.[16] OLEDs using these emitters showed EQE_{max} of 10% and CIE at (0.15, 0.07). Since this report, other analogues based on DPS acceptors have been reported, many reaching EQE_{max} values in excess of 10%.[34-38] Employing a related TADF emitter based on a dibenzo-fused phosphacycle acceptor produced a somewhat poorer performance in the device, with EQE_{max} of 4.9% and CIE at (0.15, 0.16).[39] Hatakeyama *et al*.[40] designed an interesting class of deep-blue TADF emitters based on a "multiple resonance effect", which produced narrow-band emission spectra with CIE at (0.13, 0.09) and an EQE_{max} of 13.5%. A second generation emitter by the same group showed improved performance with EQE_{max} of 18.3% and CIE at (0.13, 0.11).[41] Cui *et al*.[42] synthesized a series of deep-blue TADF emitters based on a carbazole donor and a diphenyltriazine acceptor and achieved an EQE_{max} of 19.2% with CIE at (0.15, 0.10). Wada *et al*.[43] adapted an earlier emitter design of Hirata *et al.*[29] by the incorporation of adamantyl groups on the triazine acceptor to afford deep-blue TADF emitter for solution-processed OLEDs, showing EQE_{max} of 11.2% and CIE at (0.15, 0.13) while Woo *et al*.[44] have

modified the donor groups to both increase emission energy, as well as achieving preferential horizontal transition dipole orientation of the emitters in the film in order to enhance light outcoupling; achieving devices with EQE_{max} of 7.7% and CIE at (0.15, 0.08). Komatsu *et al.*[45] developed related pyrimidine-based emitters with EQE_{max} of 18% and CIE at (0.16,0.15). Seo *et al.*[46] employed an indolocarbazole moiety as the acceptor in the design of their deep-blue TADF emitters, which achieved an EQE of 19.5% with CIE at (0.15, 0.16). Lee *et al.*[47] demonstrated that by placing a carbazole donor *ortho* to a dimesitylborane acceptor, a very high EQE_{max} of 22.6% with CIE of (0.14, 0.15) could be achieved. When both orientation in the film and photoluminescence quantum yield can be optimized, outstanding device performance can result, as demonstrated by Rajamalli *et al.*,[48] who produced OLEDs with EQE_{max} of 31.9% and CIE of (0.14, 0.18) based on a dipyridylketone acceptor design. Recently, a deep-blue emitter bearing two carbazole donors ortho to the cyanobenzene acceptor was reported by Chan *et al.*,[49] where OLEDs achieved EQE_{max} of 10.3% and CIE at (0.16, 0.06). The device performances of the aforementioned work together with this study are summarized in Table **1**.

Table **1**. Summary of reported deep-blue TADF device performances and this work.

Emitter	**EQE_{max} (%)**	**EQE @ 100 cd m^{-2} (%)**	**CIE**	**Ref.**
2CzdOXD4MeOPh	6.6	2.0	(0.15, 0.11)	This work
3	10	~2.5	(0.15, 0.07)	16
DMOC-DPS	14.5	9.0	(0.16, 0.16)	34
DTC-mBPSB	5.5	---	(0.15, 0.08)	35
DMTDAc	19.8	19.8	(0.15, 0.13)	36
DTPPDDA	4.7	2.2	(0.15, 0.09)	37
G2	--- (4.1 cd A^{-1})[a]	---	(0.15, 0.12)	38
MFAc-OPO	4.9	~0.6	(0.15, 0.16)	39
DABNA-1	13.5	~6	(0.13, 0.09)	40
B2	18.3	12.6	(0.13, 0.11)	41

Cz-TRZ3	19.2	---	(0.15, 0.10)	42
FA-TA	11.2	---	(0.15, 0.13)	43
DTXSAF	7.7	~5	(0.15, 0.08)	44
Ac-3MHPM	18	10.4	(0.16, 0.15)	45
ICzDAc	19.5	---	(0.15, 0.16)	46
CzoB	22.6	18.4	(0.14, 0.15)	47
3DPyM-pDTC	31.9	26.1	(0.14, 0.18)	48
DCzBN3	10.3	5.4	(0.16, 0.06)	49
[a] EQE not reported.				

In this study, a series of four deep blue to sky blue TADF emitters have been synthesized and characterized whose structures are shown in Chart **1**. These molecules possess the same scaffold as the dicarbazoyldicyanobenzene (**2CzPN**) reported by Uoyama *et al.*[15] but with the replacement of the cyano groups by the less electron-withdrawing oxadiazole units. The rationale for our design is three-fold. Firstly, the weaker acceptor strength of oxadiazoles[50-51] compared with cyano groups will translate into a bluer emission, presuming that the intramolecular charge transfer (ICT) nature of emission is conserved. Secondly, oxadiazoles show promising thermal stability and electron injection and transporting properties.[50,52-57] Lastly, according to theoretical calculations, the LUMO density of **2CzPN** is mostly located on the central benzene ring[15] whereas that of oxadiazole is located on the heterocyclic ring (*vide infra*).[50,54] This implies that the electron density of the HOMO, which in this study is localized on the carbazole units, and LUMO in the oxadiazole derivatives should be more separated than in **2CzPN**; however, the weaker strength of the oxadiazole acceptor results in greater delocalization of the electron density of the LUMO onto the benzene bridge thus resulting in comparable ΔE_{ST} to the reference emitter.

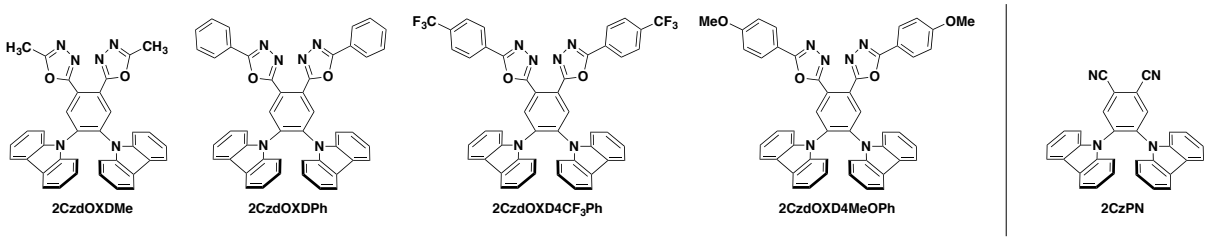

Chart **1**. Left: Oxadiazole TADF emitters in this study. Right: Reference emitter **2CzPN**

Results and Discussion

Synthesis

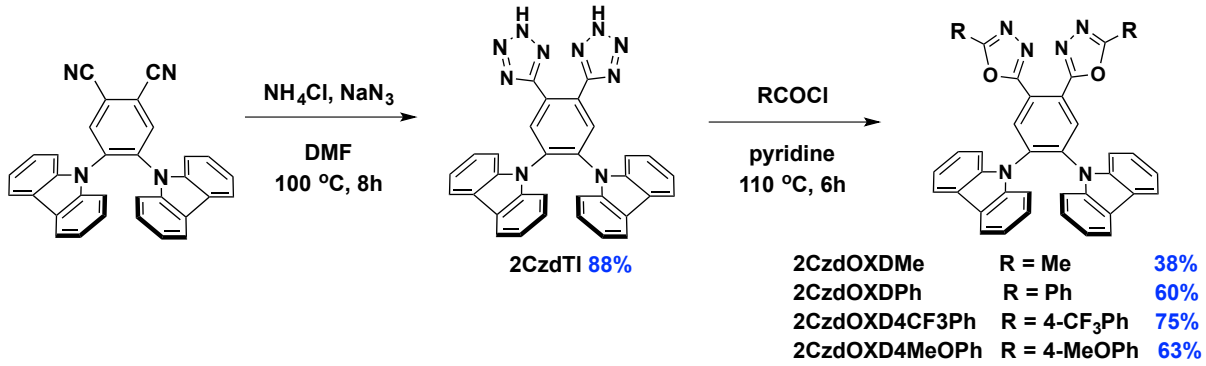

Scheme **1**. Synthesis of oxadiazole-based emitters.

The synthetic route for the four oxadiazole emitters is shown in Scheme **1**, starting from the reference emitter **2CzPN**, which is itself obtained in a much improved yield of 80% compared to the one originally reported by Uoyama *et al.* (8.5%) using a similar protocol.[15] Despite the many synthetic routes available for the installation of the oxadiazole moiety,[58-60] a two-step protocol passing through a ditetrazole intermediate (**2CzdTl**) [59] was found to be most straightforward given the presence of the cyano groups. As a result, **2CzPN** was reacted with ammonium chloride and NaN_3 in DMF at 120 ºC overnight to afford **2CzdTl** in 88% yield. The key for the success of this reaction is the isolation of **2CzdTl**, which can be precipitated from the reaction mixture as a white solid by pouring the reaction mixture into a 1M HCl solution. The ease of isolation of **2CzdTl** permits facile multigram scale up of the target materials. Following isolation, **2CzdTl** can then be reacted with the corresponding acid

chloride of choice to provide the desired oxadiazole emitters in good yield (38-75%). All four oxadiazole emitters were found to be thermally stable beyond 300 °C by TGA; 2CzdOXDMe and 2CzdOXDPh melt at 308 and 310 °C, respectively while 2CzdOXD4CF_3Ph and 2CzdOXD4MeOPh melt at 274 and 260 °C, respectively (For TGA, DTA and DSC traces see: Figures S28-S39).

Absorption and Electrochemistry

Table **2**. Summary of absorption and electrochemistry of oxadiazole emitters and **2CzPN** as control.

Emitter	λ_{abs}[a] (nm), [ε ($\times 10^4$ M^{-1} cm^{-1})]	Electrochemistry[b] (eV)
2CzdOXDMe	281 [2.26], 290 [2.46], 321 [1.37], 335 [1.51], 353 [1.36]	HOMO: -5.83 LUMO: -2.70 ΔE: 3.13
2CzdOXDPh	258 [5.38], 283 [4.39], 291 [4.48], 320 [2.38], 333 [2.20], 361 [2.12]	HOMO: -5.84 LUMO: -2.80 ΔE: 3.04
2CzdOXD4CF_3Ph	257 [4.81], 283 [4.36], 291 [4.45], 319 [2.00], 332 [1.95], 367 [1.79]	HOMO: -5.84 LUMO: -2.86 ΔE: 2.98
2CzdOXD4MeOPh	256 [4.10], 290 [4.72], 334 [2.45], 353 [2.12]	HOMO: -5.88 LUMO: -2.74 ΔE: 3.14
2CzPN	280(sh) [1.72], 289 [2.14], 319 [1.02], 329 [1.17], 364 [1.14][c]	HOMO: -5.88 LUMO: -2.97 ΔE: 2.91
2CzPN[d]	367[e]	HOMO: -5.89 LUMO: -2.97 ΔE: 2.92

[a] in DCM at 298 K. [b] in MeCN with 0.1 M [nBu$_4$N]PF_6 as the supporting electrolyte and Fc/Fc^+ as the internal reference. The HOMO and LUMO energies were calculated using the relation $E_{HOMO/LUMO} = -(E^{ox}_{pa,1} / E^{red}_{pc,1} + 4.8)$eV, where E^{ox}_{pa} and E^{red}_{pc} are anodic and cathodic peak potentials respectively. $\Delta E = -(E_{HOMO}-E_{LUMO})$.[61] [c] in MeCN at 298K. [d] Values from Ref [62]. [e] Only longest wavelength peak reported, in MeCN.

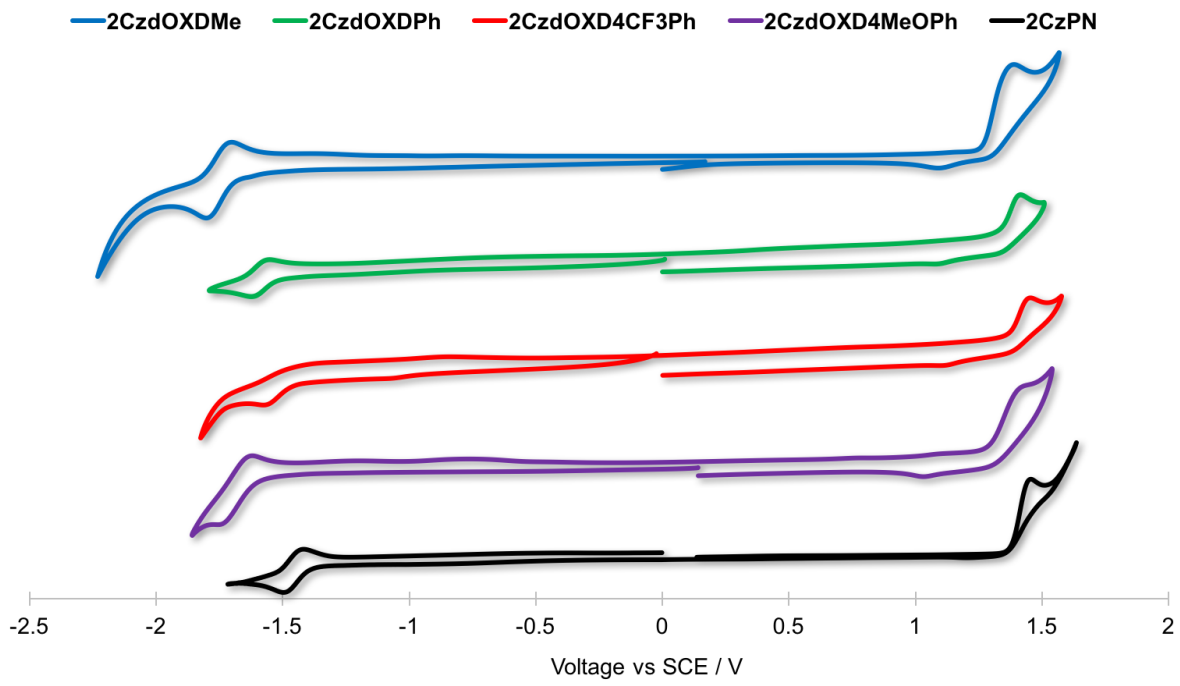

Figure **1**. CVs of the TADF emitters in degassed MeCN under argon with 0.1 M [*n*Bu$_4$N]PF$_6$ as the supporting electrolyte and using Fc/Fc$^+$ as the internal standard. The CVs are reported *vs* SCE.

The electrochemistry of the TADF emitters was studied by CV in degassed MeCN solutions under argon, Figure **1**. The HOMO levels are expectedly nearly identical (Table **2**, -5.83 to -5.88 eV), the result of the very similar orbital delocalization patterns over the carbazole donors and the central phenyl bridge as shown by Density Functional Theory (DFT) calculations (*vide infra*). The LUMO levels of the different emitters are, however, strongly influenced by the acceptor strength induced by the groups attached to the oxadiazole acceptors. The LUMO level of **2CzdOXDPh** is lower by 0.1 eV compared to **2CzdOXDMe** as a result of increased conjugation length afforded by the phenyl group. Compound **2CzdOXD4CF$_3$Ph** has the most stabilized LUMO (-2.86 eV) due to the strong electron-withdrawing effect of the trifluoromethyl group while **2CzdOXD4MeOPh** has the shallowest LUMO (-2.74 eV) due to the strong mesomerically electron-donating effect of methoxy group. For each emitter, the oxidation is irreversible, which is not unexpected as carbazole radical cations are known to be

electrochemically unstable and undergo dimerization.[63-64] Conversely, only **2CzdOXD4CF$_3$Ph** shows an irreversible reduction, probably due to cleavage of the C-F bonds.[65-66] The result of the use of the oxadiazole acceptors is an increase in the electrochemical gap from 2.91 eV for **2CzPN** to between 2.98-3.14 eV for the four TADF emitters.

Photophysical Properties

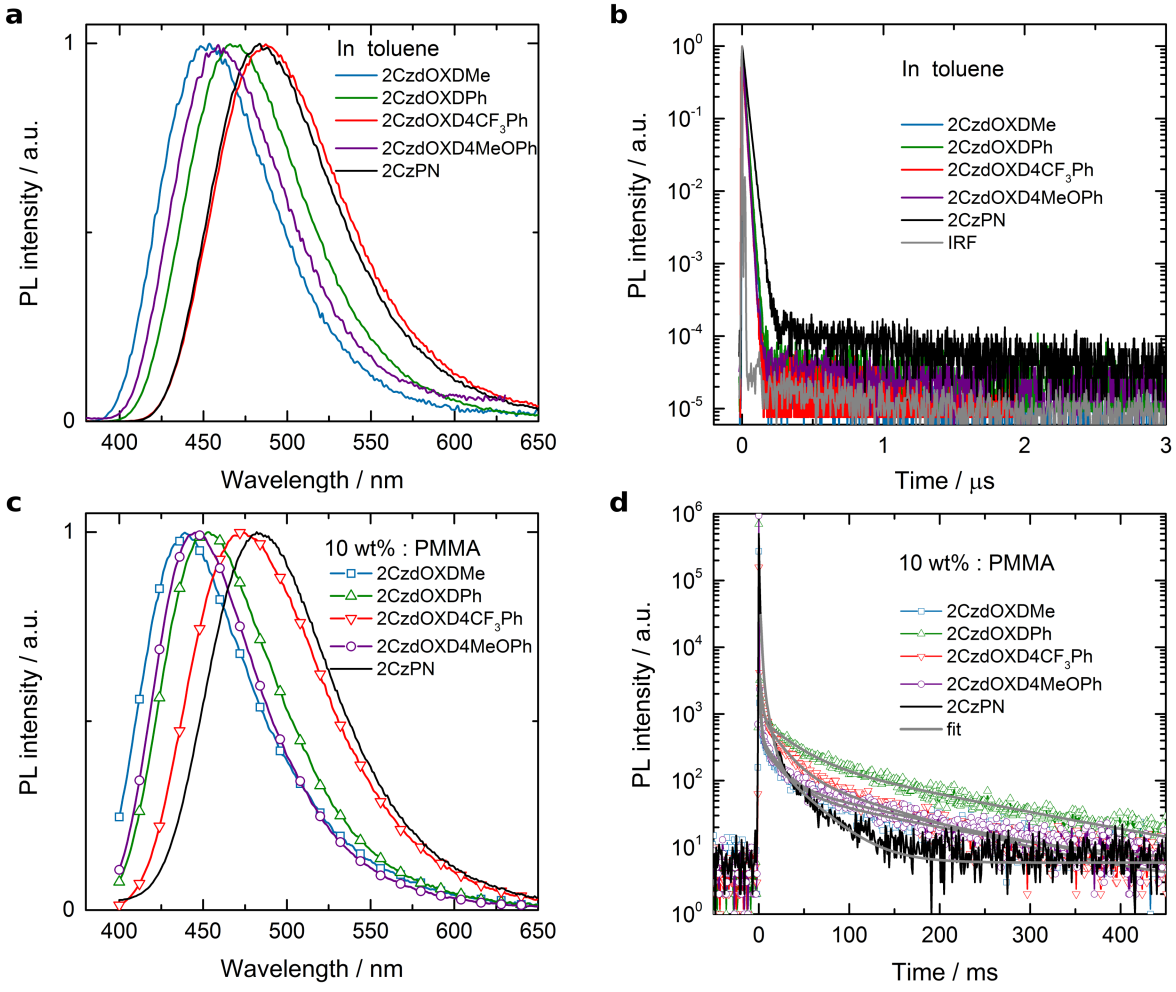

Figure **2**. a) Emission spectra (λ_{exc} = 340 nm) and b) decay profiles (λ_{exc} = 378 nm) of the TADF emitters in degassed toluene at RT; c) Steady-state photoluminescence spectra of emitters embedded in a PMMA matrix at 10 wt% (λ_{exc} = 378 nm); d) Photoluminescence decay of emitters embedded in PMMA matrix at 10 wt% (λ_{exc} = 378 nm).

Table **3.** Summary of solution and thin film photophysical properties of the oxadiazole TADF emitters and **2CzPN** as reference.

	PhMe			Thin Film[c]		
	λ_{PL}[a] /nm	Φ_{PL}[b] /%	τ_{PL} /ns	λ_{PL}[a] /nm	Φ_{PL}[d] /%	τ_{PL} /ns[e]
2CzdOXDMe	453 (79)	28.7 (24.5)	14.5	439 (77)	46.4 (39.6)	11.8, $3.0\cdot10^6$ (75%), $40.0\cdot10^6$ (19%)
2CzdOXDPh	466 (82)	38.3 (27.5)	15.6	453 (81)	62.0 (54.5)	11.0, $4.9\cdot10^6$ (63%), $45.2\cdot10^6$ (27%)
2CzdOXD4CF$_3$Ph	487 (90)	39.1 (25.7)	19.1	474 (94)	74.9 (57.1)	11.6, $2.3\cdot10^6$ (77%), $23.2\cdot10^6$ (19%)
2CzdOXD4MeOPh	459 (78)	47 (46.7)	13.1	447 (73)	41.1 (37.7)	11.5, $1.5\cdot10^6$ (83%), $17.3\cdot10^6$ (10%)
2CzPN	484 (85)	28.1 (26.2)	24.4 (99.5%)/1122 (0.5%)	492 (83)	76.0 (62.6)	18.4, $1.2\cdot10^6$ (90%), $4.8\cdot10^6$ (10%)

[a.] Emission maxima and full-width at half maximum (FWHM) are reported from degassed solutions. FWHM in parentheses. [b.] 0.5M quinine sulfate in H_2SO_4 (aq) was used as reference (PLQY: 54.6%).[67] Values quoted are in degassed solutions. Values in parentheses are for aerated solutions. [c.] Thin films were prepared by spin-coating doped samples in PMMA (10 wt%). [d.] Values determined using an integrating sphere under an N_2 atmosphere as described above in the main text. Values in parentheses are for samples measured in air. [e.] Prompt lifetimes determined from the monoexponential fit of the initial decay by TCSPC; delayed lifetimes determined from the bi-exponential decay by MCS, weighting corresponding to the pre-exponential factors are indicated in parentheses.

The solution-state photophysical properties of the four oxadiazole emitters were studied in toluene (Figure **2a**), DCM and MeCN. The photophysical data for PhMe are reported in Table **3**. All four emitters show positive solvatochromism and broad and unstructured emission profiles,[59,68-69] which are characteristic of emission from an ICT state. The broadness of emission also increases with increasing polarity of the solvent. Regardless of solvent, the wavelength at emission maximum increases in the order: **2CzdOXDMe** < **2CzdOXD4MeOPh** < **2CzdOXDPh** < **2CzdOXD4CF$_3$Ph** (Figure S**41**), which is consistent with the correspondingly decreasing bandgaps obtained from electrochemistry.

We envisioned that the weaker acceptor strength of the oxadiazole compared to the cyano group would cause a desired blue-shift in the emission in our emitters with respect to **2CzPN**. Indeed, the LUMO levels of the four oxadiazole compounds range from -2.70 eV to -2.86 eV while the LUMO of **2CzPN** was determined to be -2.97 eV (Table **2**), and their emission was blue-shifted as a consequence. For example, **2CzdOXDMe** has an emission maximum at 453 nm in toluene, blue-shifted by 31 nm (1414 cm^{-1}) compared with **2CzPN** (484 nm) in the same solvent.

The photoluminescence quantum yields (Φ_{PL}) in degassed solutions range from 28 to 47% and do not significantly change with solvent choice. The Φ_{PL} values in degassed solutions are always higher than those in aerated solutions. This finding provides direct evidence for transient population of the triplet excited state, which is sensitive to triplet oxygen quenching and is diagnostic of TADF materials.[69-72] The emission lifetime of **2CzPN** in toluene consists of a prompt (24.4 ns) and a weak delayed component (1.12 μs, 0.5% amplitude in multi-exponential fit). The prompt component in the oxadiazole-containing compounds in toluene is

faster (13-19 ns); however, the delayed component is too weak to be resolved as it coincides with the instrument response function (Figure **2b**, grey line). Thus, the delayed fluorescence in all of the studied compounds in toluene is smaller than we can reliably detect.

To assess the viability of these oxadiazole emitters in OLED devices, their photophysical properties were investigated in the solid state. Thin films were prepared by spin-coating 10 wt % DCM solution of emitter in PMMA (Figure **2c**). All emission maxima are blue-shifted by ~15 nm and the profiles generally slightly sharper compared with those measured in toluene solution. The thin film Φ_{PL} (40-75%) are significantly higher than in solution as a result of the more rigid environment that constrains the torsional motion thereby reducing the non-radiative decay rate.[73] In particular, **2CzdOXDPh** (λ_{PL} = 453 nm) and **2CzdOXD4CF$_3$Ph** (λ_{PL} = 474 nm) exhibit remarkable Φ_{PL} values of 62% and 75% in the deep-blue region under nitrogen, making them very promising blue TADF materials for OLEDs. Similar to their behavior in solution, the Φ_{PL} of the thin films are higher under a nitrogen atmosphere than when exposed to air, confirming the presence of TADF in solid state. Similar to the solution-state emission spectra, the thin film emission spectra of the four oxadiazole emitters were blue-shifted compared to that of **2CzPN**. Figure **2d** shows the corresponding PL decay curves. For each of the emitters, there is a fast prompt decay ($\tau_p \approx 10$ ns) and several very long delayed emission components. The dominant delayed components, τ_d, were estimated to be τ_{d1} = 3.0 ms (75%, amplitude in multi-exponential fit to data) and τ_{d2} = 40 ms (19%) for compounds **2CzdOXDMe**, τ_{d1} = 4.9 ms (63%) and τ_{d2} = 45.2 ms (27%) for **2CzdOXDPh**, τ_{d1} = 2.3 ms (77%) and τ_{d2} = 23.2 ms (19%) for **2CzdOXD4CF$_3$Ph**, and τ_{d1} = 1.5 ms (83%) and τ_{d2} = 17 ms (10%) for **2CzdOXD4MeOPh**.

For device applications, 1,3-bis(carbazol-9-yl)benzene (mCP) and 2,8-bis(diphenylphosphoryl) dibenzo[b,d] thiophene (PPT) hosts were selected, due to their hole or electron transporting ability, respectively, in combination with the high triplet energy (E_T = 2.9 eV and 3.0 eV for mCP[74] and PPT[75], respectively). Figure **3** and Table **4** summarize the photophysical properties of the emitters embedded in vacuum-deposited mCP or PPT matrices. Due to the high singlet energies of these matrices, Förster energy back-transfer cannot occur and the emission of the doped films originates solely from the dopant (Figure **S42**). The Φ_{PL} values of the emitters embedded in mCP or PPT remain relatively high, ranging from 14 to 55%. They are, however, lower compared to the Φ_{PL} recorded in PMMA films. The singlet-triplet gap, ΔE_{ST}, of each of the emitters was estimated from the difference in the onset of the fluorescence and phosphorescence spectra recorded at 77K (Figure **3a**). Overall, the compounds exhibit experimentally determined ΔE_{ST} that are comparable to **2CzPN**,[76] and range from 0.30 to 0.46 eV (Figure **3b**), which are in line with the theoretical calculations (*vide infra*). All of the compounds showed prompt and delayed emission in the vacuum-deposited films (Figure **3c**). The spectroscopic evidence signifies that the four oxadiazole compounds are indeed TADF emitters.

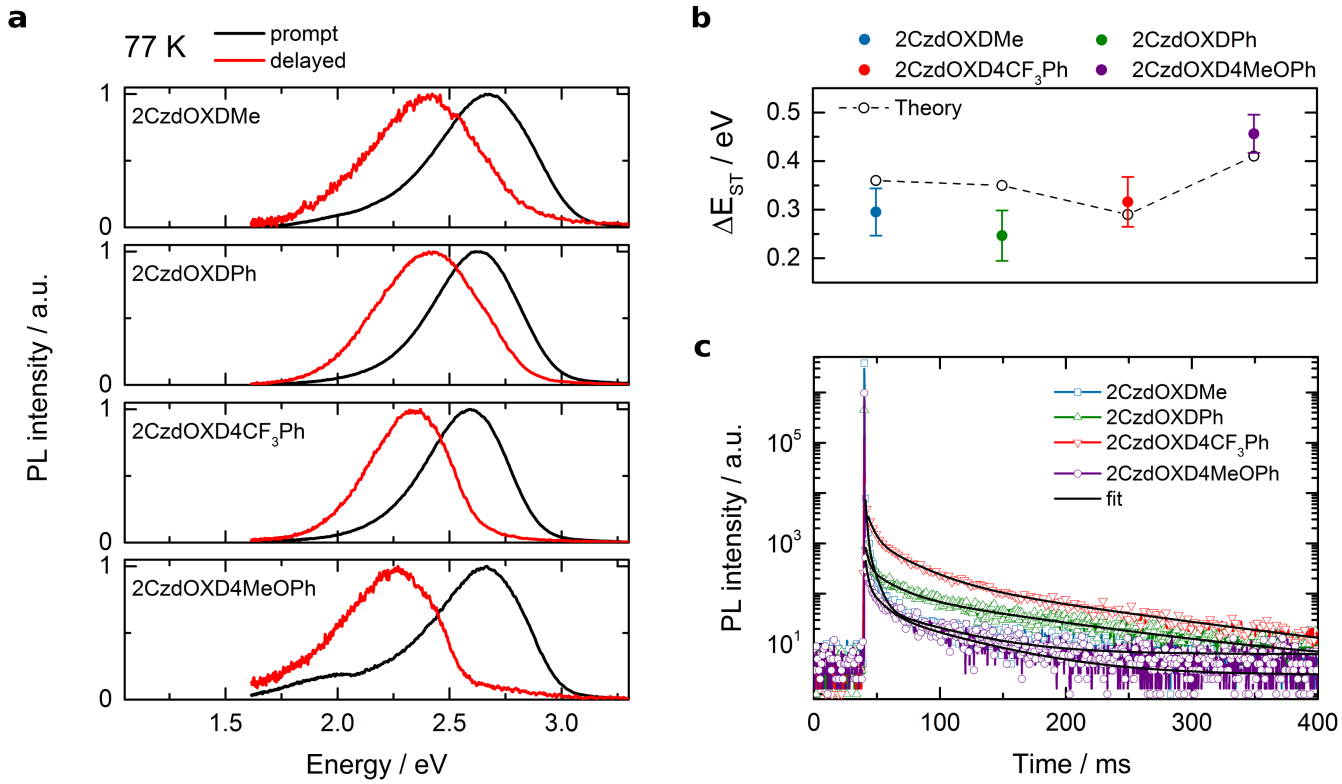

Figure **3**. a) Prompt and delayed spectra of emitters embedded in mCP (2CzdOXDMe and 2CzdOXDMeOPh) or PPT (2CzdOXDPh and 2CzdOXD4CF$_3$PH) hosts at 6 wt%. Measurements are performed at 77 K. b) Summary of the ΔE_{ST} values estimated from the onset of fluorescence and phosphorescence spectra and compared to the DFT calculations. c) Corresponding PL decay curves at room temperature (λ_{exc} = 378 nm).

Table **4.** Summary of thin film photophysical properties of studied compounds embedded in mCP or PPT hosts.

Film	λ_{PL} / nm	FWHM / nm	Φ_{PL}[a] / %	τ_{PL} / ns	Prompt:delayed / %	ΔE_{ST} / eV
mCP:**2CzdOXDMe**	435	73	29.3 (27.0)	5.7, 1·10^6 (86%),	92.0:8.0	0.30±0.05

				$4.8 \cdot 10^6$ (13%)		
PPT:**2CzdOXDPh**	454	85	43.9 (38.7)	9.5, $2.4 \cdot 10^6$ (62%), $17.8 \cdot 10^6$ (27%)	88.2:11.8	0.25±0.05
PPT: **2CzdOXD4CF$_3$Ph**	474	83	54.9 (41.0)	6.0, $4.5 \cdot 10^6$ (67%), $25.8 \cdot 10^6$ (28%),	74.6:25.4	0.32±0.05
mCP:**2CzdOXD4MeOPh**	449	77	14.9 (14.1)	8.1, $1.7 \cdot 10^6$ (69%), $10.1 \cdot 10^6$ (23%),	95.1:4.9	0.46±0.04

[a] Values in parentheses are for aerated samples.

Theoretical Calculations

Further characterization of the optoelectronic properties of these compounds has been carried on with the help of DFT calculations. To do so, we used the methodology developed by Moral *et al.* offering a particularly accurate description of the electronic structure of materials for OLED applications.[77] Not surprisingly, the HOMO energies of the different compounds remain almost constant as in each case the HOMO is localized on the carbazole moiety (Figure **4**). These are ca. 0.1 eV more stabilized than the HOMO for 2CzPN, indicating

that the nature of the acceptor moiety modestly modulates the HOMO. The LUMO energies on the other hand decrease significantly, showing that the synthetic approach allows for near-independent tuning of the frontier orbital energies upon replacing cyano groups in 2CzPN with oxadiazole acceptors. Not surprisingly, the replacement of cyano groups with oxadiazoles results in a more delocalized LUMO for the four oxadiazole derivatives while the HOMO remains mainly localized on the carbazole groups and the central phenyl ring (Figure **4**).

Expectedly, because of the lower electron-withdrawing character of methyl-substituted oxadiazole, **2CzdOXDMe** possesses the highest energy LUMO in the series, more than 0.4 eV destabilized compared to **2CzPN**, resulting in a significantly bluer emission (see S_1 energy in Table **5**). Replacing the methyl group with phenyl as is the case in **2CzdOXDPh** results in a more modest 0.24 eV destabilization of the LUMO compared to **2CzPN**. Interestingly, by grafting CF_3-substituted phenyl groups to the oxadiazole units, the LUMO energy of **2CzdOXD4CF$_3$Ph** is stabilized with respect to **2CzdOXDPh** and in fact is close to that of **2CzPN**; conversely the LUMO energy of **2CzdOXD4MeOPh** is destabilized relative to **2CzdOXDPh**.

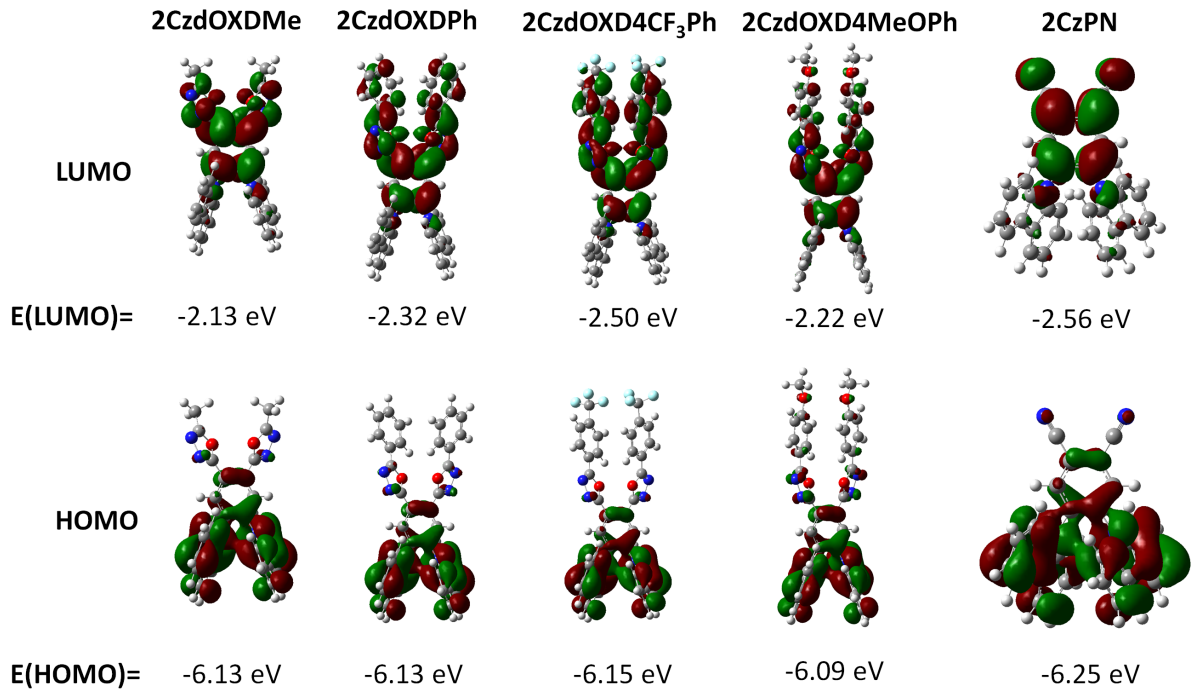

Figure **4.** Frontier orbitals contour plots and energies of the different derivatives as well as **2CzPN** considering acetonitrile as a solvent.

The calculations are able to predict the emission colors of both **2CzPN** and the four oxadiazole derivatives. Specifically, the S_1 energies of **2CzdOXDMe** appears as the bluest while **2CzdOXD4CF$_3$Ph** is slightly red-shifted compared to **2CzPN**. All molecules exhibit similar electronic structure with T_2 lying in between T_1 and S_1.

We note that an additional T_3 excited state lies below S_1 in **2CzdOXD4MeOPh**. Considering the electronic structure, the up-conversion to S_1 could potentially arise either directly from T_1 or from an intermediate triplet excited state after reverse internal conversion. The T_1 and S_1 excited states are mainly characterized by HOMO to LUMO transitions with a pronounced intramolecular charge-transfer (ICT) character. Interestingly, the singlet-triplet splitting, ΔE_{ST}, moderately decreases when going from **2CzdOXDMe** to **2CzdOXD4CF$_3$Ph**, in line with a slight decrease of the oscillator strength. We further characterize the degree of

spatial separation between occupied (ϕ_i) and virtual (ϕ_a) molecular orbitals, Δr, relative to a particular excited state by evaluating the averaged hole-electron distance based on the computation of the detachment and attachment centroids radius vectors and the calculation of the distance between them using the NANCY_EX package.[78-80] We mention that this approach appears to be perfectly equivalent[78] to the one we used previously and which is based on the corresponding centroid of the Natural Transition Orbitals involved in the studied excited-state transition.[77]

A cutoff $\Delta r > 1.5-2.0$ Å has been proposed previously to both distinguish, and characterize, a charge-transfer excitation,[81] and it was shown that the magnitude of the ΔE_{ST} is inversely proportional to Δr.[77] Recently, it has been demonstrated that in order to obtain TADF emitters with very small ΔE_{ST}, both Δr relative to the excitation from S_0 to T_1 [$\Delta r(T_1)$] and S_1 [$\Delta r(S_1)$] should be large, and in particular the triplet component was found to play a dominant role in determining ΔE_{ST} of the different compounds studied.[82] When examining Δr in Table **5**, all Δr reported confirm the expected ICT character that could be inferred from the orbital localization (Figure **4**). Among all the compounds, **2CzPN** and **2CzdOXD4CF$_3$Ph** show the largest $\Delta r(T_1)$ and exhibit the smallest ΔE_{ST} while **2CzdOXD4MeOPh** shows the largest ΔE_{ST} and smallest $\Delta r(T_1)$, in agreement with what was proposed by Huang and co-workers .[82]

Table **5.** Excitation energies, ΔE_{ST}, oscillator strengths and compositions of the excited states in terms of monoelectronic transitions (molecular orbitals) for **2CzPN** and its derivatives.

Compound	States	Energy (eV)	O.S. (a.u.)	Main MO component of the transitions from S_0 (%)	Δr (Å)
2CzdOXDMe	T_1	2.88	-	HOMO → LUMO (80.9%)	2.40

	S_1	3.24	0.13	HOMO → LUMO (97.9%)	3.82
	$\Delta E(S_1\text{-}T_1)$	**0.36**			-
2CzdOXDPh	T_1	2.75	-	HOMO → LUMO (75.7%)	2.43
	S_1	3.10	0.12	HOMO → LUMO (97%)	4.37
	$\Delta E(S_1\text{-}T_1)$	**0.35**			-
2CzdOXD4CF$_3$Ph	T_1	2.68	-	HOMO → LUMO (76.9%)	3.12
	S_1	2.97	0.10	HOMO → LUMO (95.8%)	4.91
	$\Delta E(S_1\text{-}T_1)$	**0.29**			-
2CzdOXD4MeOPh	T_1	2.76	-	HOMO → LUMO (71.4%)	1.24
	S_1	3.17	0.13	HOMO → LUMO (97.2%)	3.73
	$\Delta E(S_1\text{-}T_1)$	**0.41**			
2CzPN	T_1	2.67	-	HOMO → LUMO (87.7%)	2.80
	S_1	2.98	0.11	HOMO → LUMO (96.5%)	3.70
	$\Delta E(S_1\text{-}T_1)$	**0.31**			-

Crystal structures

Suitable crystals for X-ray analysis were obtained for all of **2CzdOXDMe**, **2CzdOXDPh**, **2CzdOXD4CF$_3$Ph** and **2CzdOXD4MeOPh**, as well as for the reference compound **2CzPN** (Figure **5**). Crystals of **2CzdOXDMe** and **2CzPN** were grown by the slow evaporation of mixed solutions of toluene/hexane, crystals of **2CzdOXD4CF$_3$Ph** by the slow evaporation of mixed solutions of toluene/MeCN, while crystals of **2CzdOXDPh** and **2CzdOXD4MeOPh** were grown by the vapour diffusion of Et_2O into concentrated solutions of 1,2-dichloroethane (**2CzdOXDPh**) or dichloromethane (**2CzdOXD4MeOPh**). All four new compounds exhibit similar conformations, with both carbazole rings disposed in a highly twisted arrangement with respect to the plane of the central benzene [dihedral angles of 58.51(3)–67.64(7)°]. In comparison to the structure of **2CzPN**,[83] the carbazole units in **2CzdOXDMe**, **2CzdOXDPh**, **2CzdOXD4CF$_3$Ph** and **2CzdOXD4MeOPh** are closer to orthogonal to the central benzene [**2CzPN** dihedral angles of 50.60(4)–60.83(4)°]. The oxadiazole heterocycles in the four emitters are less restrained in the orientations they can occupy due to their smaller size, and

show a much wider range of dihedral angles relative to the central benzene than the carbazole fragments, with a general pattern of having one oxadiazole ring close to coplanar with the benzene, and one close to orthogonal [dihedral angles 6.18(8)–21.77(10) for more coplanar rings, and 49.32(5)–78.11(11)° for more orthogonal]. In **2CzdOXDPh**, **2CzdOXD4CF$_3$Ph** and **2CzdOXD4MeOPh**, the oxadiazole moiety and its aryl substituent are approximately coplanar [dihedral angles of 4.04(9)–28.27(6)°], indicative of a degree of conjugation between these ring systems in the solid-state structures. Additionally, one further distinction is seen in the structures. For **2CzdOXDMe** and **2CzdOXDPh**, the oxadiazoles are oriented such that they are aligned closer to parallel than antiparallel, whereas for **2CzdOXD4CF$_3$Ph** and **2CzdOXD4MeOPh**, the converse is the case.

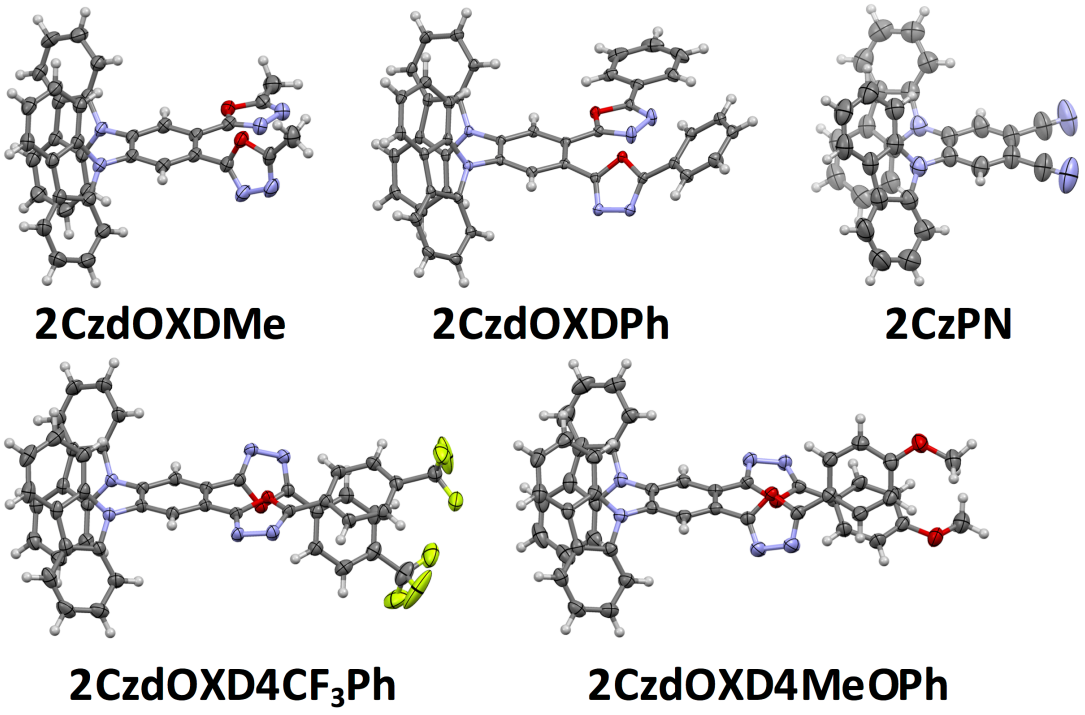

Figure **5**. Structures of **2CzdOXDMe**, **2CzdOXDPh**, **2CzdOXD4CF$_3$Ph**, **2CzdOXD4MeOPh**, and **2CzPN** (50% probability ellipsoids; co-crystallized solvent molecules omitted). Heteroatoms: N, light blue; F, green; and O, red.

Organic Light-Emitting Diodes

The four oxadiazole emitters were then integrated into OLED devices. Figure **6** shows the architecture employed to build sky-blue to deep-blue OLEDs. The general device structure consisted of indium tin oxide ITO (90 nm)/NPB (35 nm)/mCP (10 nm)/EML (15 nm)/PPT (10 nm)/TmPyPB (30 nm)/LiF (1 nm)/Al (100 nm). NPB is *N,N*'-bis(naphthalen-1-yl)-*N,N*'-bis(phenyl)-benzidine and acts as the hole transport layer. TmPyPB is 1,3,5-tri(*m*-pyrid-3-yl-phenyl)benzene and acts as the electron transporting layer (ETL). Devices **1-5** comprising different emission layers (EMLs) incorporating the oxadiazole emitters were built, and these were compared to a reference Device **R1**, based on **2CzPN**. The Device **R1** was based on the device stack reported by Adachi and co-workers:[76] ITO (90 nm)/NPB (35 nm)/mCP (10 nm)/ **2CzPN**:mCP (6 wt%, 15nm)/PPT (10 nm)/TPBi (40 nm)/LiF (1 nm)/Al (100 nm). Here, the ETL used was TPBi, which is 1,3,5-tris(1-phenyl-1H-benzimidazol- 2-yl) benzene. The thin layer of 10 nm mCP (PPT) before (after) the EML in all of the devices acts as the electron (hole) blocking layer.

The EML of Device **1** consisted of **2CzdOXDMe**:mCP (6 wt%). Devices **2** and **3** comprised **2CzdOXDPh**:PPT (6 wt%) and **2CzdOXD4CF$_3$Ph**:PPT (6 wt%) as their EMLs. For **2CzdOXD4MeOPh**, devices employing both mCP (Device **4**) and PPT (Device **5**) as hosts were fabricated. The reason for using mCP for **2CzdOXDMe** is that the LUMO level of **2CzdOXDMe** (-2.7 eV) matches the LUMO of PPT,[76] and thus efficient electron trapping by the dopant would

not be achieved in a PPT matrix. On the other hand, mCP is predominantly hole conductive[74,84] and hole injection and conduction is more efficient compared to electron transport in the mCP device. Therefore, better charge balance within the EML was expected when using PPT as a host and thus PPT was used as a matrix material for emitters **2CzdOXDPh** and **2CzdOXD4CF$_3$Ph**. Due to the intermediate LUMO value of **2CzdOXD4MeOPh** (-2.74 eV), it was tested in both mCP and PPT.

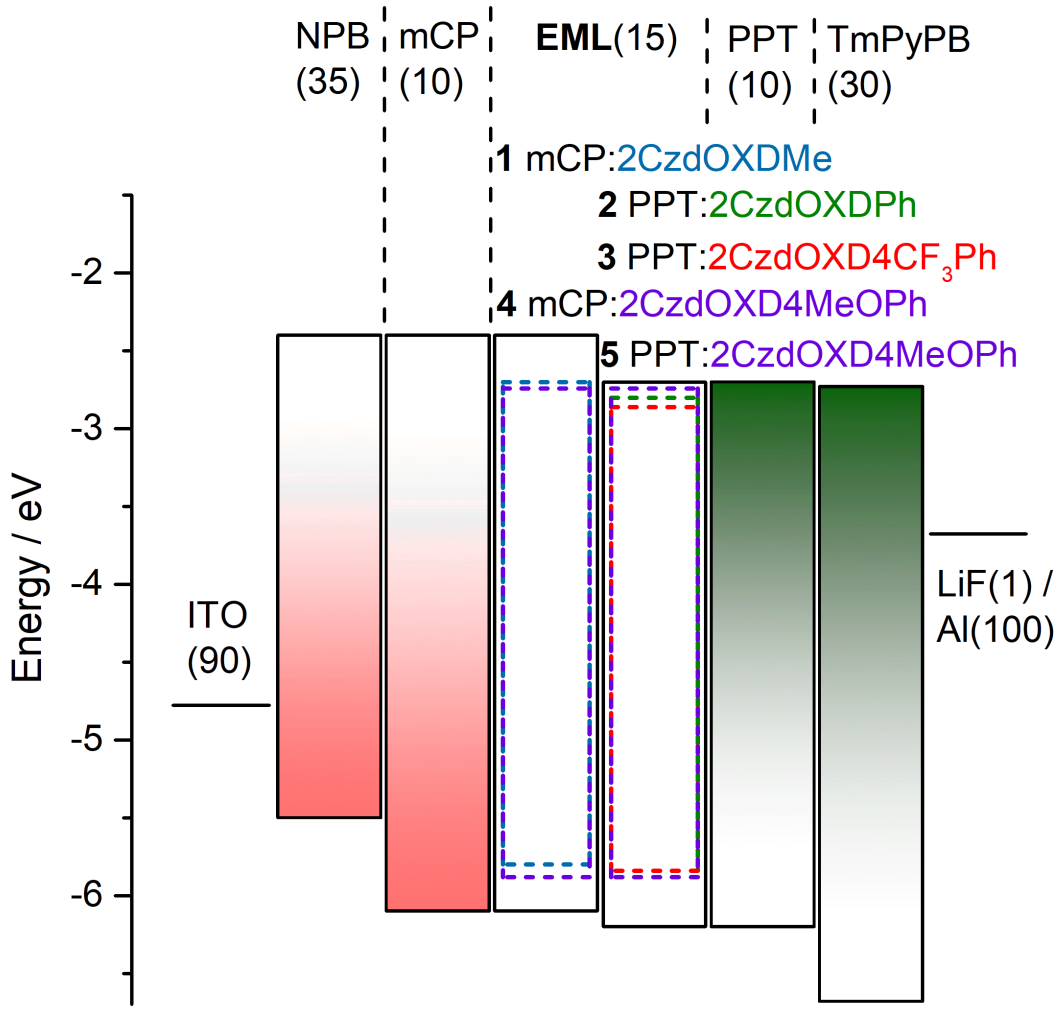

Figure **6.** Functional layer sequence of the devices **1**-**5** comprising oxadiazole emitters.

Figure **7** and Table **6** summarise the OLED performance. The electroluminescence (EL) spectra shift systematically from sky-blue emission exhibited by Device **R1** and Device **3** (λ_{EL} = 480 nm and 474 nm, respectively) to deep-blue emission exhibited by Devices **1**, **2**, **4** and **5**,

with corresponding peak emission at λ_{EL} = 446 nm, 455 nm, 446 nm and 448 nm, respectively (Figure **7a**). In agreement with photophysical data (Tables **3** and **4**), devices fabricated with **2CzdOXD4CF$_3$Ph** (Device **3**) demonstrated the most red-shifted electroluminescence compared with the other three oxadiazole emitters due to the presence of the electron-withdrawing CF_3 groups, which result in **2CzdOXD4CF$_3$Ph** possessing the deepest LUMO (-2.86 eV, Table **2**) among all oxadiazole emitters. In general, the electroluminescence spectra of the oxadiazole emitters agree very well with photoluminescence spectra obtained from their thin films doped in mCP or PPT hosts (Table **4**) and the trend of their emission energies can be correlated to their corresponding LUMO levels (Table **2**). Devices **2** and **3** show the highest turn-on voltages V_{on} of 4.30 V and 4.60 V, respectively, and flat current-voltage characteristic (Figure **7b**). This could be indicative of high series resistance due to poor charge injection and transport when using **2CzdOXDPh** and **2CzdOXD4CF$_3$Ph** doped PPT system as the EMLs. On the other hand, Devices **1**, **4** and **5**, show steep current-voltage characteristics (Figure **7b**) and V_{on} of 3.85 V, 4.15 V and 4.05 V, respectively.

Figure **7c** shows the external quantum efficiency (EQE) versus the current density of the OLEDs. Device **3** reaches a maximum EQE_{max} of 11.2% at low brightness, indicating the presence of an efficient triplet harvesting via the TADF mechanism (Figure **7c**). However, the EQE of **3** drops by almost a factor of five to 2.5% at 100 cd m^{-2}. Similar trends of relatively high EQE at low brightness (4.7%, 6.8%, 6.6% and 4.2% for Devices **1**, **2**, **4**, and **5,** respectively) and a strong efficiency roll-off are also observed for the other devices. Such efficiency roll-off might be caused by the bimolecular annihilation reactions due to the presence of the long-lived triplet states (τ_{PL} ranging from 1.0 to 25.8 ms), as evidenced from the photophysical studies of the thin films of oxadiazole emitters doped in mCP or PPT hosts (Table **4**). The most severe efficiency roll-off was observed for Devices **2** and **3**, comprising emitters **2CzdOXDPh** and

2CzdOXD4CF$_3$Ph, respectively, with the corresponding critical current densities j_{crit} in the range of 0.05 mA cm^{-2}. Here, j_{crit} denotes the current density at which the EQE drops to half of its maximum value. In comparison, the lowest roll-off was observed for the device with **2CzdOXDMe** as the emitter, device **1** (j_{crit} = 13 mA cm^{-2}). The average delayed lifetime (τ_{avg}) of emitters **2CzdOXDPh** and **2CzdOXD4CF$_3$Ph** and **2CzdOXDMe** is indicative of the triplet state lifetime in these compounds and is estimated to be 6.3 ms, 10.2 ms and 1.5 ms, respectively (Table **4**). The shorter τ_{avg} leads to the less pronounced efficiency roll-off, in line with the bimolecular annihilation pathway being the limiting factor for efficient OLED operation at high current density and brightness. Thus, further work on optimising exciton dynamics in the EML and minimizing bimolecular annihilation reactions is needed. Additionally, it is important to note that the reference device **R1** used in this work does not represent the optimal device structure for the sky-blue emitter **2CzPN**. Indeed, the selection of the functional layer sequence is crucial to minimize the electrical losses in blue TADF OLEDs. For example, Zhang *et al.*[85] showed that replacing TPBi with diphenylphosphine oxide-based ETLs that exhibit high electron mobility and high E_T can enhance the **2CzPN**-based OLED performance up to EQE_{max} = 17.4%. Replacement of mCP as the EBL with a higher hole mobility and thermal stability material 3,5-di(9H-carbazol-9-yl)-*N,N*-diphenylaniline (DCDPA)[86] has been shown to increase the efficiency further to EQE_{max} = 19.2%.[87] Finally, Sun *et al.*[88] fabricated OLEDs comprising a mixed host layer for the TADF dopant to boost the performance further to 21.8%, which was also shown to be the efficiency limit for **2CzPN**-based devices. Similar improvements are thus expected to enhance device performance when oxadiazole emitters are used. Nevertheless, this work demonstrates that a systematic shift toward deep-blue electroluminescence is possible by replacing the CN accepting groups in 2CzPN by oxadiazole unit containing moieties. Figure **7d** shows the corresponding color coordinates of Devices **1**-**5** in comparison to the reference

Device **R1**. Devices **1**, **2**, **4**, and **5** all exhibit CIE x,y coordinates < 0.2 and, thus, are well suited as deep blue emitters.

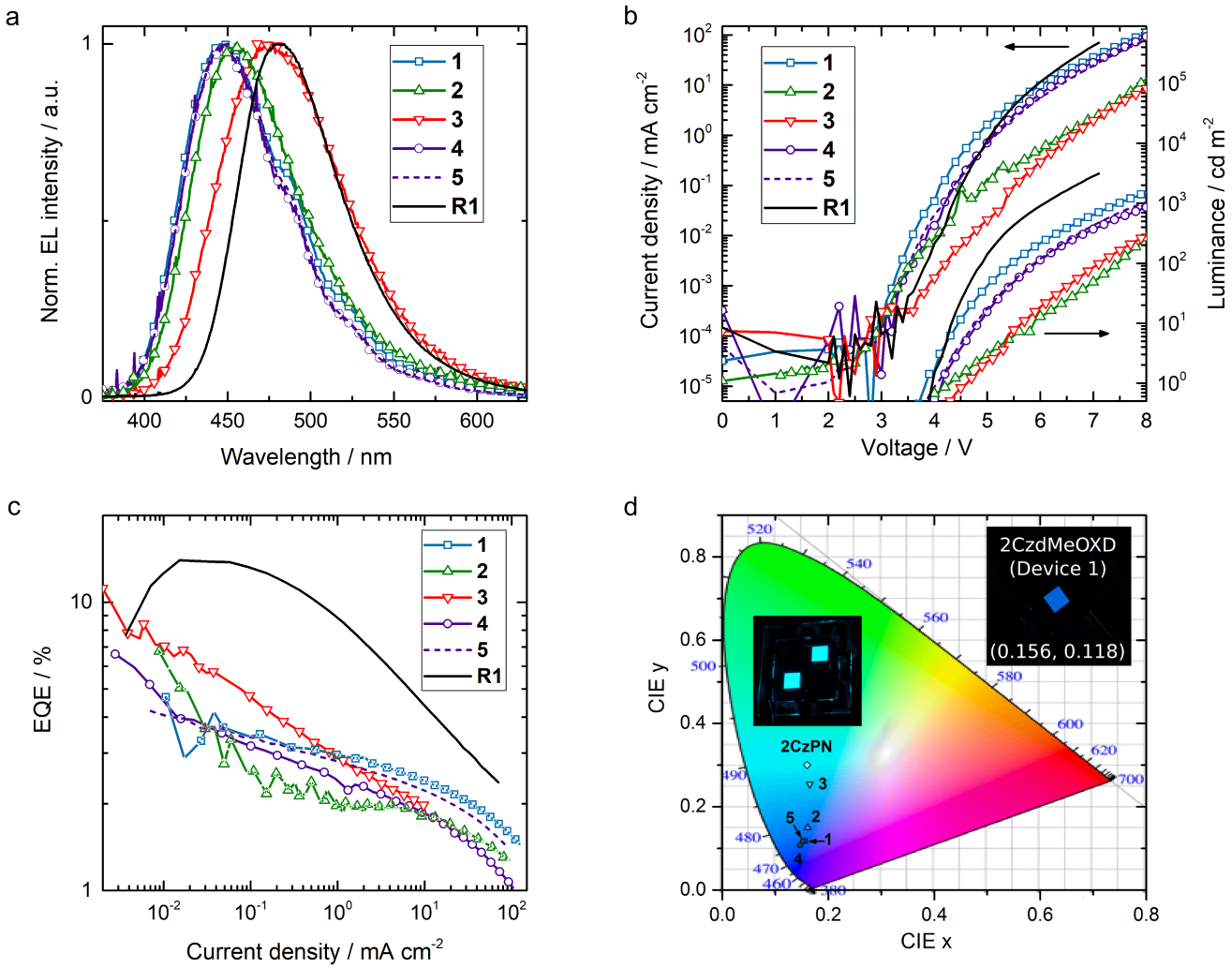

Figure **7.** OLED performance of devices based on sky-blue to deep-blue emitters. **a**) Electroluminescence spectra; **b**) current density-voltage-luminance characteristics; **c**) external quantum efficiency dependence on current density; **d**) CIE color coordinates of devices **1-5** and Device **R1** based on **2CzPN** for comparison. Inset shows photographs of Device **1** and Device **R1**.

Table **6.** Summary of OLED performances.

Emitter	Host	V_{on} / V [a]	λ_{EL}/ nm	FWHM / nm	CIE (x, y)	$EQE_{max}/EQE_{100}/EQE_{1000}$ / % [b]	PE_{max} / lm W^{-1}	CE_{max} / cd A^{-1}
2CzdOXDMe	mCP	3.85	446	78	(0.156, 0.118)	4.7 / 2.6 / 1.8	3.7	4.2
2CzdOXDPh	PPT	4.30	455	75	(0.161, 0.150)	6.8 / 2.0 / 1.4	5.9	7.5
2CzdOXD4CF$_3$Ph	PPT	4.60	474	78	(0.165, 0.254)	11.2 / 2.5 / - [c]	14.5	18.9

2CzdOXD4MeOPh	mCP	4.15	446	73	(0.147, 0.108)	6.6 / 2.0 / 0.8	5.0	5.7
2CzdOXD4MeOPh	PPT	4.05	448	73	(0.153, 0.118)	4.2 / 2.4 / 1.5	3.2	3.8
2CzPN	mCP	3.95	480	71	(0.160, 0.300)	14.0 / 10.3 / 4.0	18.4	25.9

[a.] Defined as the lowest operating voltage at the luminance of >1 cd m^{-2}; [b.] Max = Maximum value, 100 = measured at 100 cd m^{-2}, 1000 = measured at 1000 cd m^{-2}; [c.] 1000 cd m^{-2} not reached.

Conclusions

This study shows the viability of using oxadiazole acceptor units to blue-shift the emission while conserving the TADF properties of the emitters in the solid-state. Compared to **2CzPN**, the replacement of the nitrile acceptors for oxadiazole units destabilized the LUMO level while keeping the HOMO essentially unchanged, which was observed both experimentally and corroborated by DFT calculations, causing an increase in the emission energy. The TADF nature of the compounds was confirmed by a combination of oxgygen-dependence measurements on the photoluminescence quantum yield, time-resolved measurements clearly showing prompt and delayed components in the film. The experimentally measured and calculated ΔE_{ST} are in strong agreement. OLED devices using **2CzdOXD4MeOPh** produced deep blue light with CIE coordinates of (0.147, 0.108) and maximum external quantum efficiency of 6.6% while a more efficient (EQE_{max} of 11.2%) sky-blue device was fabricated (0.165, 0.254) with **2CzdOXD4CF$_3$Ph**. The efficiencies obtained are demonstrative of TADF being operational in the OLED devices. In future, the observed strong roll-off of the devices needs to be addressed using improved device design.

Acknowledgements. EZ-C thanks the University of St Andrews for support. We are grateful to the EPSRC for financial support (grants EP/P010482/1, EP/J01771X and EP/J00916). IDWS is a Royal Society Wolfson Research Merit Award Holder. We thank the EPSRC UK National

Mass Spectrometry Facility at Swansea University for analytical services. CM acknowledges funding by the European Commission through a Marie Skłodowska Curie Individual Fellowship (No. 703387).

Supporting Information. Complete experimental protocol. NMR spectra. HR-mass spectra. HPLC traces. CIF files. (CCDC: 1852947-1852950, 1436867) for **2CzdOXDMe**, **2CzdOXDPh**, **2CzdOXD4CF$_3$Ph**, **2CzdOXD4MeOPh**, and **2CzPN**. Supplementary photophysical data. Supplementary computations and coordinates.

References.

(1) Baldo, M. A.; O'Brien, D. F.; You, Y.; Shoustikov, A.; Sibley, S.; Thompson, M. E.; Forrest, S. R., Highly Efficient Phosphorescent Emission from Organic Electroluminescent Devices. *Nature* **1998**, *395*, 151-154.
(2) Yersin, H.; Rausch, A. F.; Czerwieniec, R.; Hofbeck, T.; Fischer, T., The Triplet State of Organo-Transition Metal Compounds. Triplet Harvesting and Singlet Harvesting for Efficient OLEDs. *Coord. Chem. Rev.* **2011**, *255*, 2622-2652.
(3) Plummer, E. A.; van Dijken, A.; Hofstraat, J. W.; De Cola, L.; Brunner, K., Electrophosphorescent Devices Based on Cationic Complexes: Control of Switch-on Voltage and Efficiency Through Modification of Charge Injection and Charge Transport. *Adv. Funct. Mater.* **2005**, *15*, 281-289.
(4) Lamansky, S.; Djurovich, P.; Murphy, D.; Abdel-Razzaq, F.; Lee, H.-E.; Adachi, C.; Burrows, P. E.; Forrest, S. R.; Thompson, M. E., Highly Phosphorescent Bis-Cyclometalated Iridium Complexes: Synthesis, Photophysical Characterization, and Use in Organic Light Emitting Diodes. *J. Am. Chem. Soc.* **2001**, *123*, 4304-4312.
(5) Adachi, C.; Baldo, M. A.; Thompson, M. E.; Forrest, S. R., Nearly 100% Internal Phosphorescence Efficiency in an Organic Light Emitting Device. *J. Appl. Phys.* **2001**, *90*, 5048-5051.
(6) Xiao, L.; Chen, Z.; Qu, B.; Luo, J.; Kong, S.; Gong, Q.; Kido, J., Recent Progresses on Materials for Electrophosphorescent Organic Light-Emitting Devices. *Adv. Mater.* **2011**, *23*, 926-952.
(7) Choy, W. C. H.; Chan, W. K.; Yuan, Y., Recent Advances in Transition Metal Complexes and Light-Management Engineering in Organic Optoelectronic Devices. *Adv. Mater.* **2014**, *26*, 5368-5399.
(8) Sasabe, H.; Kido, J., Development of High Performance OLEDs for General Lighting. *J. Mater. Chem. C* **2013**, *1*, 1699-1707.
(9) Gather, M. C.; Köhnen, A.; Meerholz, K., White Organic Light-Emitting Diodes. *Adv. Mater.* **2011**, *23*, 233-248.
(10) Wong, M. Y.; Zysman-Colman, E., Purely Organic Thermally Activated Delayed Fluorescence Materials for Organic Light-Emitting Diodes. *Adv. Mater.* **2017**, *29*, 1605444.
(11) Yang, Z.; Mao, Z.; Xie, Z.; Zhang, Y.; Liu, S.; Zhao, J.; Xu, J.; Chi, Z.; Aldred, M. P., Recent Advances in Organic Thermally Activated Delayed Fluorescence Materials. *Chem. Soc. Rev.* **2017**, *46*, 915-1016.
(12) Li, Y.; Liu, J.-Y.; Zhao, Y.-D.; Cao, Y.-C., Recent Advancements of High Efficient Donor–acceptor Type Blue Small Molecule Applied for OLEDs. *Mater. Today* **2017**, *20*, 258-266.
(13) Liu, Y.; Li, C.; Ren, Z.; Yan, S.; Bryce, M. R., All-organic Thermally Activated Delayed Fluorescence Materials for Organic Light-emitting Diodes. *Nat. Rev. Mater.* **2018**, *3,* 18020.

(14) Bui, T. T.; Goubard, F.; Ibrahim-Ouali, M.; Gigmes, D.; Dumur, F., Recent Advances on Organic Blue Thermally Activated Delayed Fluorescence (TADF) Emitters for Organic Light-emitting Diodes (OLEDs). *Beilstein J. Org. Chem.* **2018**, *14*, 282-308.
(15) Uoyama, H.; Goushi, K.; Shizu, K.; Nomura, H.; Adachi, C., Highly efficient Organic Light-emitting Diodes from Delayed Fluorescence. *Nature* **2012**, *492*, 234-238.
(16) Zhang, Q.; Li, J.; Shizu, K.; Huang, S.; Hirata, S.; Miyazaki, H.; Adachi, C., Design of Efficient Thermally Activated Delayed Fluorescence Materials for Pure Blue Organic Light Emitting Diodes. *J. Am. Chem. Soc.* **2012**, *134*, 14706-14709.
(17) Taneda, M.; Shizu, K.; Tanaka, H.; Adachi, C., High Efficiency Thermally Activated Delayed Fluorescence Based on 1,3,5-tris(4-(diphenylamino)phenyl)-2,4,6-tricyanobenzene. *Chem. Commun.* **2015**, *51*, 5028-5031.
(18) Czerwieniec, R.; Yu, J.; Yersin, H., Blue-light Emission of Cu(I) Complexes and Singlet Harvesting. *Inorg. Chem.* **2011**, *50*, 8293-8301.
(19) Czerwieniec, R.; Kowalski, K.; Yersin, H., Highly Efficient Thermally Activated Fluorescence of a New Rigid Cu(I) Complex [Cu(dmp)(phanephos)]+. *Dalton. Trans.* **2013**, *42*, 9826-9830.
(20) Linfoot, C. L.; Leitl, M. J.; Richardson, P.; Rausch, A. F.; Chepelin, O.; White, F. J.; Yersin, H.; Robertson, N., Thermally Activated Delayed Fluorescence (TADF) and Enhancing Photoluminescence Quantum Yields of [Cu(I)(diimine)(diphosphine)](+) Complexes-photophysical, Structural, and Computational Studies. *Inorg. Chem.* **2014**, *53*, 10854-10861.
(21) Leitl, M. J.; Krylova, V. A.; Djurovich, P. I.; Thompson, M. E.; Yersin, H., Phosphorescence Versus Thermally Activated Delayed Fluorescence. Controlling Singlet-triplet Splitting in Brightly Emitting and Sublimable Cu(I) Compounds. *J. Am. Chem. Soc.* **2014**, *136*, 16032-16038.
(22) Osawa, M.; Kawata, I.; Ishii, R.; Igawa, S.; Hashimoto, M.; Hoshino, M., Application of Neutral d10 Coinage Metal Complexes with an Anionic Bidentate Ligand in Delayed Fluorescence-type Organic Light-emitting Diodes. *J. Mater. Chem. C* **2013**, *1*, 4375- 4383.
(23) Chen, X.-L.; Lin, C.-S.; Wu, X.-Y.; Yu, R.; Teng, T.; Zhang, Q.-K.; Zhang, Q.; Yang, W.-B.; Lu, C.-Z., Highly Efficient Cuprous Complexes with Thermally Activated Delayed Fluorescence and Simplified Solution Process OLEDs using the Ligand as Host. *J. Mater. Chem. C* **2015**, *3*, 1187-1195.
(24) Wallesch, M.; Volz, D.; Zink, D. M.; Schepers, U.; Nieger, M.; Baumann, T.; Brase, S., Bright Coppertunities: Multinuclear Cu(I) Complexes with N-P Ligands and their Applications. *Chem. Eur. J.* **2014**, *20*, 6578-6590.
(25) Mehes, G.; Nomura, H.; Zhang, Q.; Nakagawa, T.; Adachi, C., Enhanced Alectroluminescence Efficiency in a Spiro-acridine Derivative Through Thermally Activated Delayed Fluorescence. *Angew. Chem. Int. Ed. Engl.* **2012**, *51*, 11311-11315.
(26) Xu, S.; Liu, T.; Mu, Y.; Wang, Y.-F.; Chi, Z.; Lo, C.-C.; Liu, S.; Zhang, Y.; Lien, A.; Xu, J., An Organic Molecule with Asymmetric Structure Exhibiting Aggregation-Induced Emission, Delayed Fluorescence, and Mechanoluminescence. *Angew. Chem. Int. Ed.* **2015**, *54*, 874-878.
(27) Jankus, V.; Data, P.; Graves, D.; McGuinness, C.; Santos, J.; Bryce, M. R.; Dias, F. B.; Monkman, A. P., Highly Efficient TADF OLEDs: How the Emitter-Host Interaction Controls Both the Excited State Species and Electrical Properties of the Devices to Achieve Near 100% Triplet Harvesting and High Efficiency. *Adv. Funct. Mater.* **2014**, *24*, 6178-6186.
(28) Nakagawa, T.; Ku, S. Y.; Wong, K. T.; Adachi, C., Electroluminescence Based on Thermally Activated Delayed Fluorescence Generated by a Spirobifluorene Donor-acceptor Structure. *Chem. Commun.* **2012**, *48*, 9580-9582.
(29) Hirata, S.; Sakai, Y.; Masui, K.; Tanaka, H.; Lee, S. Y.; Nomura, H.; Nakamura, N.; Yasumatsu, M.; Nakanotani, H.; Zhang, Q.; Shizu, K.; Miyazaki, H.; Adachi, C., Highly Efficient Blue Electroluminescence Based on Thermally Activated Delayed Fluorescence. *Nat. Mater.* **2015**, *14*, 330-336.
(30) Zhang, Y.; Lee, J.; Forrest, S. R., Tenfold Increase in the Lifetime of Blue phosphorescent Organic Light-emitting Diodes. *Nat. Commun.* **2014**, *5*, 5008.
(31) Udagawa, K.; Sasabe, H.; Cai, C.; Kido, J., Low-driving-voltage Blue Phosphorescent Organic Light-Emitting Devices with External Quantum Efficiency of 30%. *Adv. Mater.* **2014**, *26*, 5062-5066.

(32) Reineke, S.; Lindner, F.; Schwartz, G.; Seidler, N.; Walzer, K.; Lussem, B.; Leo, K., White Organic Light-emitting Diodes with Fluorescent Tube Efficiency. *Nature* **2009**, *459*, 234-238.
(33) Yang, X.; Xu, X.; Zhou, G., Recent Advances of the Emitters for High Performance Deep-blue Organic Light-emitting Diodes. *J. Mater. Chem. C* **2015**, *3*, 913-944.
(34) Wu, S.; Aonuma, M.; Zhang, Q.; Huang, S.; Nakagawa, T.; Kuwabara, K.; Adachi, C., High-efficiency Deep-blue Organic Light-emitting Diodes Based on a Thermally Activated Delayed Fluorescence Emitter. *J. Mater. Chem. C* **2014**, *2*, 421-424.
(35) Liu, M.; Seino, Y.; Chen, D.; Inomata, S.; Su, S. J.; Sasabe, H.; Kido, J., Blue Thermally Activated Delayed Fluorescence Materials Based on Bis(phenylsulfonyl)benzene Derivatives. *Chem. Commun.* **2015**, *51*, 16353-16356.
(36) Lee, I.; Lee, J. Y., Molecular Design of Deep Blue Fluorescent Emitters with 20% External Quantum Efficiency and Narrow Emission Spectrum. *Org. Electron.* **2016**, *29*, 160-164.
(37) Sun, J. W.; Baek, J. Y.; Kim, K.-H.; Huh, J.-S.; Kwon, S.-K.; Kim, Y.-H.; Kim, J.-J., Azasiline-based Thermally Activated Delayed Fluorescence Emitters for Blue Organic Light Emitting Diodes. *J. Mater. Chem. C* **2017**, *5*, 1027-1032.
(38) Li, J.; Liao, X.; Xu, H.; Li, L.; Zhang, J.; Wang, H.; Xu, B., Deep-blue Thermally Activated Delayed Fluorescence Dendrimers with Reduced Singlet-triplet Energy Gap for Low Roll-off Non-doped Solution-processed Organic Light-emitting Diodes. *Dyes and Pigments* **2017**, *140*, 79-86.
(39) Lee, J.; Aizawa, N.; Yasuda, T., Molecular Engineering of Phosphacycle-based Thermally Activated Delayed Fluorescence Materials for Deep-blue OLEDs. *J. Mater. Chem. C* **2018**, DOI: 10.1039/C1037TC05709A.
(40) Hatakeyama, T.; Shiren, K.; Nakajima, K.; Nomura, S.; Nakatsuka, S.; Kinoshita, K.; Ni, J.; Ono, Y.; Ikuta, T., Ultrapure Blue Thermally Activated Delayed Fluorescence Molecules: Efficient HOMO–LUMO Separation by the Multiple Resonance Effect. *Adv. Mater.* **2016**, *28*, 2777-2781.
(41) Matsui, K.; Oda, S.; Yoshiura, K.; Nakajima, K.; Yasuda, N.; Hatakeyama, T., One-Shot Multiple Borylation toward BN-Doped Nanographenes. *J. Am. Chem. Soc.* **2018**, *140*, 1195-1198.
(42) Cui, L. S.; Nomura, H.; Geng, Y.; Kim, J. U.; Nakanotani, H.; Adachi, C., Controlling Singlet-Triplet Energy Splitting for Deep-Blue Thermally Activated Delayed Fluorescence Emitters. *Angew. Chem. Int. Ed. Engl.* **2017**, *56*, 1571-1575.
(43) Wada, Y.; Kubo, S.; Kaji, H., Adamantyl Substitution Strategy for Realizing Solution-Processable Thermally Stable Deep-Blue Thermally Activated Delayed Fluorescence Materials. *Adv. Mater.* **2018**, *30,* 1705641.
(44) Woo, S.-J.; Kim, Y.; Kim, M.-J.; Baek, J. Y.; Kwon, S.-K.; Kim, Y.-H.; Kim, J.-J., Strategies for the Molecular Design of Donor–Acceptor-type Fluorescent Emitters for Efficient Deep Blue Organic Light Emitting Diodes. *Chem. Mater.* **2018**, *30*, 857-863.
(45) Komatsu, R.; Ohsawa, T.; Sasabe, H.; Nakao, K.; Hayasaka, Y.; Kido, J., Manipulating the Electronic Excited State Energies of Pyrimidine-Based Thermally Activated Delayed Fluorescence Emitters To Realize Efficient Deep-Blue Emission. *ACS Appl Mater Interfaces* **2017**, *9*, 4742-4749.
(46) Seo, J. A.; Im, Y.; Han, S. H.; Lee, C. W.; Lee, J. Y., Unconventional Molecular Design Approach of High-Efficiency Deep Blue Thermally Activated Delayed Fluorescent Emitters Using Indolocarbazole as an Acceptor. *ACS Appl Mater Interfaces* **2017**, *9*, 37864-37872.
(47) Lee, Y. H.; Park, S.; Oh, J.; Shin, J. W.; Jung, J.; Yoo, S.; Lee, M. H., Rigidity-Induced Delayed Fluorescence by Ortho Donor-Appended Triarylboron Compounds: Record-High Efficiency in Pure Blue Fluorescent Organic Light-Emitting Diodes. *ACS Appl Mater Interfaces* **2017**, *9*, 24035-24042.
(48) Rajamalli, P.; Senthilkumar, N.; Huang, P. Y.; Ren-Wu, C. C.; Lin, H. W.; Cheng, C. H., New Molecular Design Concurrently Providing Superior Pure Blue, Thermally Activated Delayed Fluorescence and Optical Out-Coupling Efficiencies. *J. Am. Chem. Soc.* **2017**, *139*, 10948-10951.
(49) Chan, C.-Y.; Cui, L.-S.; Kim, J. U.; Nakanotani, H.; Adachi, C., Rational Molecular Design for Deep-Blue Thermally Activated Delayed Fluorescence Emitters. *Adv. Funct. Mater.* **2018**, *28*, 1706023.

(50) Zhang, Y.; Zuniga, C.; Kim, S.-J.; Cai, D.; Barlow, S.; Salman, S.; Coropceanu, V.; Brédas, J.-L.; Kippelen, B.; Marder, S., Polymers with Carbazole-Oxadiazole Side Chains as Ambipolar Hosts for Phosphorescent Light-Emitting Diodes. *Chem. Mater.* **2011**, *23*, 4002-4015.
(51) Li, B.; Zhou, L.; Cheng, H.; Huang, Q.; Lan, J.; Zhou, L.; You, J., Dual-emissive 2-(2-Hydroxyphenyl)oxazoles for High Performance Organic Electroluminescent Devices: Discovery of a New Equilibrium of Excited State Intramolecular Proton Transfer with a Reverse Intersystem Crossing Process. *Chem. Sci.* **2018**, *9*, 1213-1220.
(52) Tao, Y.; Wang, Q.; Yang, C.; Wang, Q.; Zhang, Z.; Zou, T.; Qin, J.; Ma, D., A Simple Carbazole/oxadiazole Hybrid Molecule: an Excellent Bipolar Host for Green and Red Phosphorescent OLEDs. *Angew. Chem. Int. Ed. Engl.* **2008**, *47*, 8104-8107.
(53) Wu, X.; Wang, L.; Hua, Y.; Wang, C.; Batsanov, A. S.; Bryce, M. R., A Carbazole–oxadiazole Diad Molecule for Single-emitting-component White Organic Light-emitting devices (WOLEDs). *Tetrahedron* **2014**, *70*, 2015-2019.
(54) Li, Q.; Cui, L. S.; Zhong, C.; Jiang, Z. Q.; Liao, L. S., Asymmetric Design of Bipolar Host Materials with Novel 1,2,4-Oxadiazole Unit in Blue Phosphorescent Device. *Org. Lett.* **2014**, *16*, 1622-1625.
(55) Gong, S.; Fu, Q.; Zeng, W.; Zhong, C.; Yang, C.; Ma, D.; Qin, J., Solution-Processed Double-Silicon-Bridged Oxadiazole/Arylamine Hosts for High-Efficiency Blue Electrophosphorescence. *Chem. Mater.* **2012**, *24*, 3120-3127.
(56) Zhang, D.; Cao, X.; Wu, Q.; Zhang, M.; Sun, N.; Zhang, X.; Tao, Y., Purely Organic Materials for Extremely Simple all-TADF White OLEDs: A New Carbazole/oxadiazole Hybrid Material as a Dual-role Non-doped Light Blue Emitter and Highly Efficient Orange Host. *J. Mater. Chem. C* **2018**, DOI: 10.1039/c1037tc04969b.
(57) Chidirala, S.; Ulla, H.; Valaboju, A.; Kiran, M. R.; Mohanty, M. E.; Satyanarayan, M. N.; Umesh, G.; Bhanuprakash, K.; Rao, V. J., Pyrene-Oxadiazoles for Organic Light-Emitting Diodes: Triplet to Singlet Energy Transfer and Role of Hole-Injection/Hole-Blocking Materials. *J .Org. Chem.* **2016**, *81*, 603-614.
(58) Zhang, J.; Zhou, L.; Al-Attar, H. A.; Shao, K.; Wang, L.; Zhu, D.; Su, Z.; Bryce, M. R.; Monkman, A. P., Efficient Light-Emitting Electrochemical Cells (LECs) Based on Ionic Iridium(III) Complexes with 1,3,4-Oxadiazole Ligands. *Adv. Funct. Mater.* **2013**, *23*, 4667-4677.
(59) Zheng, Y.; Batsanov, A. S.; Jankus, V.; Dias, F. B.; Bryce, M. R.; Monkman, A. P., Bipolar Molecules with High Triplet Energies: Synthesis, Photophysical, and Structural Properties. *J. Org. Chem.* **2011**, *76*, 8300-8310.
(60) Yu, W.; Huang, G.; Zhang, Y.; Liu, H.; Dong, L.; Yu, X.; Li, Y.; Chang, J., I2-mediated Oxidative C-O Bond Formation for the Synthesis of 1,3,4-Oxadiazoles from Aldehydes and Hydrazides. *J. Org. Chem.* **2013**, *78*, 10337-10343.
(61) Cardona, C. M.; Li, W.; Kaifer, A. E.; Stockdale, D.; Bazan, G. C., Electrochemical Considerations for Determining Absolute Frontier Orbital Energy Levels of Conjugated Polymers for Solar Cell Applications. *Adv. Mater.* **2011**, *23*, 2367-2371.
(62) Ishimatsu, R.; Matsunami, S.; Kasahara, T.; Mizuno, J.; Edura, T.; Adachi, C.; Nakano, K.; Imato, T., Electrogenerated Chemiluminescence of Donor–Acceptor Molecules with Thermally Activated Delayed Fluorescence. *Angew. Chem. Int. Ed.* **2014**, *53*, 6993-6996.
(63) Zotti, G.; Schiavon, G.; Zecchin, S.; Morin, J.-F.; Leclerc, M., Electrochemical, Conductive, and Magnetic Properties of 2,7-Carbazole-Based Conjugated Polymers. *Macromolecules* **2002**, *35*, 2122-2128.
(64) Tomkeviciene, A.; Grazulevicius, J. V.; Volyniuk, D.; Jankauskas, V.; Sini, G., Structure-properties Relationship of Carbazole and Fluorene Hybrid Trimers: Experimental and Theoretical Approaches. *Phys. Chem. Chem. Phys.* **2014**, *16*, 13932-13942.
(65) Coleman, J. P.; Gilde, H. G.; Utley, J. H. P.; Weedon, B. C. L., The Electrochemical Reductive Cleavage of Carbon-oxygen and Carbon-fluorine Bonds in Benzyl Systems. *J. Chem. Soc. D: Chem. Commun.* **1970**, 738-739.

(66) Inesi, A.; Rampazzo, L., Electrochemical Reduction of Halogen Containing Compounds at a Mercury Cathode: Fluoroacetic, Difluoroacetic, Trifluoroacetic acids and Corresponding Ethyl Esters in Dimethylformamide. *J. Electroanal. Chem.* **1974**, *49*, 85-93.
(67) Melhuish, W. H., Quantum Efficiences Of Fluorescence Of Organic Substances: Effect Of Solvent And Concentration Of The Fluorescent Solute 1. *J. Phys. Chem.* **1961**, *65*, 229-235.
(68) Ishimatsu, R.; Matsunami, S.; Shizu, K.; Adachi, C.; Nakano, K.; Imato, T., Solvent Effect on Thermally Activated Delayed Fluorescence by 1,2,3,5-Tetrakis(carbazol-9-yl)-4,6-dicyanobenzene. *J. Phys. Chem. A* **2013**, *117*, 5607-5612.
(69) Lee, J.; Shizu, K.; Tanaka, H.; Nomura, H.; Yasuda, T.; Adachi, C., Oxadiazole- and Triazole-based Highly-efficient Thermally Activated Delayed Fluorescence Emitters for Organic Light-emitting Diodes. *J. Mater. Chem. C* **2013**, *1*, 4599- 4604.
(70) Tanaka, H.; Shizu, K.; Miyazaki, H.; Adachi, C., Efficient Green Thermally Activated Delayed Fluorescence (TADF) from a Phenoxazine-triphenyltriazine (PXZ-TRZ) Derivative. *Chem. Commun.* **2012**, *48*, 11392-11394.
(71) Nasu, K.; Nakagawa, T.; Nomura, H.; Lin, C. J.; Cheng, C. H.; Tseng, M. R.; Yasuda, T.; Adachi, C., A Highly Luminescent Spiro-anthracenone-based Organic Light-emitting Diode Exhibiting Thermally Activated Delayed Fluorescence. *Chem. Commun.* **2013**, *49*, 10385-10387.
(72) Zhang, Q.; Kuwabara, H.; Potscavage, W. J., Jr.; Huang, S.; Hatae, Y.; Shibata, T.; Adachi, C., Anthraquinone-based Intramolecular Charge-transfer Compounds: Computational Molecular Design, Thermally Activated Delayed Fluorescence, and Highly Efficient Red Electroluminescence. *J. Am. Chem. Soc.* **2014**, *136*, 18070-18081.
(73) Lee, J.; Shizu, K.; Tanaka, H.; Nakanotani, H.; Yasuda, T.; Kaji, H.; Adachi, C., Controlled Emission Colors and Singlet-triplet Energy Gaps of Dihydrophenazine-based Thermally Activated Delayed Fluorescence Emitters. *J. Mater. Chem. C* **2015**, *3*, 2175-2181.
(74) Holmes, R. J.; Forrest, S. R.; Tung, Y.-J.; Kwong, R. C.; Brown, J. J.; Garon, S.; Thompson, M. E., Blue Organic Electrophosphorescence using Exothermic Host–guest Energy Transfer. *Appl. Phys. Lett.* **2003**, *82*, 2422-2424.
(75) Jeong, S. H.; Lee, J. Y., Dibenzothiophene Derivatives as Host Materials for High Efficiency in Deep Blue Phosphorescent Organic Light Emitting Diodes. *J. Mater. Chem.* **2011**, *21*, 14604-14609.
(76) Masui, K.; Nakanotani, H.; Adachi, C., Analysis of Exciton Annihilation in High-efficiency Sky-blue Organic Light-emitting Diodes With Thermally Activated Delayed Fluorescence. *Org. Electron.* **2013**, *14*, 2721-2726.
(77) Moral, M.; Muccioli, L.; Son, W. J.; Olivier, Y.; Sancho-García, J. C., Theoretical Rationalization of the Singlet–Triplet Gap in OLEDs Materials: Impact of Charge-Transfer Character. *J. Chem. Theory Comput.* **2015**, *11*, 168-177.
(78) Etienne, T.; Assfeld, X.; Monari, A., Toward a Quantitative Assessment of Electronic Transitions' Charge-Transfer Character. *J. Chem. Theory Comput.* **2014**, *10*, 3896-3905.
(79) Etienne, T.; Assfeld, X.; Monari, A., New Insight into the Topology of Excited States through Detachment/Attachment Density Matrices-Based Centroids of Charge. *J. Chem. Theory Comput.* **2014**, *10*, 3906-3914.
(80) Etienne, T., Probing the Locality of Excited States with Linear Algebra. *J. Chem. Theory Comput.* **2015**, *11*, 1692-1699.
(81) Guido, C. A.; Cortona, P.; Mennucci, B.; Adamo, C., On the Metric of Charge Transfer Molecular Excitations: A Simple Chemical Descriptor. *J. Chem. Theory Comput.* **2013**, *9*, 3118-3126.
(82) Chen, T.; Zheng, L.; Yuan, J.; An, Z.; Chen, R.; Tao, Y.; Li, H.; Xie, X.; Huang, W., Understanding the Control of Singlet-Triplet Splitting for Organic Exciton Manipulating: A Combined Theoretical and Experimental Approach. *Scientific Reports* **2015**, *5*, 10923.
(83) Majeed, S. A.; Ghazal, B.; Nevonen, D. E.; Goff, P. C.; Blank, D. A.; Nemykin, V. N.; Makhseed, S., Evaluation of the Intramolecular Charge-Transfer Properties in Solvatochromic and Electrochromic Zinc Octa(carbazolyl)phthalocyanines. *Inorg. Chem.* **2017**, *56*, 11640-11653.

(84) Wu, M. F.; Yeh, S. J.; Chen, C. T.; Murayama, H.; Tsuboi, T.; Li, W. S.; Chao, I.; Liu, S. W.; Wang, J. K., The Quest for High‐Performance Host Materials for Electrophosphorescent Blue Dopants. *Adv. Funct. Mater.* **2007**, *17*, 1887-1895.
(85) Zhang, Q.; Wang, B.; Tan, J.; Mu, G.; Yi, W.; Lv, X.; Zhuang, S.; Liu, W.; Wang, L., Optimized Electron-transport Material Based on m-Terphenyl-diphenylphosphine Oxide with the Harmonious Compatibility of High ET and Electron Mobility for Highly Efficient OLEDs. *J. Mater. Chem. C* **2017**, *5*, 8516-8526.
(86) Cho, Y. J.; Lee, J. Y., Low Driving Voltage, High Quantum Efficiency, High Power Efficiency, and Little Efficiency Roll-off in Red, Green, and Deep-blue Phosphorescent Organic Light-emitting Diodes Using a High-Triplet-Energy Hole Transport Material. *Adv. Mater.* **2011**, *23*, 4568-4572.
(87) Kim, G. H.; Lampande, R.; Im, J. B.; Lee, J. M.; Lee, J. Y.; Kwon, J. H., Controlling the Exciton Lifetime of Blue Thermally Activated Delayed Fluorescence Emitters Using a Heteroatom-containing Pyridoindole Donor Moiety. *Materials Horizons* **2017**, *4*, 619-624.
(88) Sun, J. W.; Kim, K. H.; Moon, C. K.; Lee, J. H.; Kim, J. J., Highly Efficient Sky-Blue Fluorescent Organic Light Emitting Diode Based on Mixed Cohost System for Thermally Activated Delayed Fluorescence Emitter (2CzPN). *ACS Appl Mater Interfaces* **2016**, *8*, 9806-9810.

GA